MEASUREMENTS OF LIFT FLUCTUATIONS DUE TO TURBULENCE

Thesis by

Philip Lamson

In Partial Fulfillment of the Requirements

For the Degree of

Doctor of Philosophy

California Institute of Technology

Pasadena, California

1956

ACKNOWLEDGMENTS

The research was carried out under the supervision of Dr. H.W. Liepmann whose encouragement and suggestions contributed greatly to its progress. Also the patient help of Dr. G.T. Skinner and Dr. A. Roshko is gratefully acknowledged.

ABSTRACT

The fluctuating lift of a rigid wing in turbulent flow is studied. The power spectra of the lift and of the turbulent fluctuations are measured. From these measurements the aerodynamic admittance of the wing is obtained.

The ratio of span/scale of turbulence is varied by means of movable end plates. For a distance between the end plates of the order of the scale of turbulence the aerodynamic admittance is expected to approach the computed values of Sears.

This is shown to be the case if the reduced frequencies are larger than $k = 0.8$. For smaller k the experimental admittance falls below Sears' values. For large ratios of span/scale of turbulence the aerodynamic admittance is decreased for all frequencies and becomes nearly independent of frequency in the investigated range $0.2 \leq k \leq 2$.

In general the measurements support the simplifying assumptions made in the statistical approach to gust loads and buffeting initiated by Clementson and by Liepmann.

TABLE OF CONTENTS

Symbols

A area under square of the absolute mechanical admittance curve

AR aspect ratio

B strength of magnet

c chord

C_L lift coefficient

F force

$f(\omega)$ angle of attack power spectrum ($f(\omega)$ is defined by the relation $\overline{\alpha^2} = \int_0^\infty f(\omega)\, d\omega$) (see References 9 and 10).

G spring constant

$g(\omega)$ lift power spectrum ($g(\omega)$ is defined by: $\overline{L^2} = \int_0^\infty g(\omega) d\omega$)

$h(\omega)$ displacement power spectrum ($h(\omega)$ is defined by: $\overline{v^2} = \int_0^\infty h(\omega) d\omega$)

i current in coil

k reduced frequency ($k = \frac{c}{2U}$)

L lift

M mesh size

m mass

s span of wing

t time

t_s span of movable strip

U mean air velocity

u component of fluctuating turbulent velocity in direction of free stream

v displacement

w component of fluctuating turbulent velocity in direction of lift vector

x	distance downstream of turbulence grid
y	spanwise coordinate
α	angle of attack
β	viscous damping constant
ω	circular frequency
ω_o	natural frequency
ν	frequency (c.p.s.)
ν_s	shedding frequency of cylinder
θ	angle hot wire anemometer makes with free stream
ϕ	aerodynamic admittance
ϕ_1	aerodynamic admittance (non-dimensional form)
ψ	mechanical admittance
χ	total admittance
λ_x	scale of turbulence in free stream direction

I. Introduction

Lift and drag of a wing or a whole configuration are usually computed on the basis of a known flight velocity U and a known angle of attack distribution α. In every practical case there will exist however random fluctuations, which one may term "noise", both in U and α.

For a rigid configuration these fluctuations are due to turbulence which may be present in the atmosphere or may be produced by part of the airplane itself. In the first case we deal with flight through a gusty atmosphere, in the second case with buffeting. Both problems belong to a class of phenomena in which a mechanical system is excited by random forces. In the case of interest here, U and α are the "input"; lift, drag or any other defined mechanical response of the airplane are to be considered the "output" of "response".

To make the problem tractable without losing its significant physical character we may assume the noise to be statistically stationary, i.e. to have statistical properties which are independent of time when averaged over a time long compared to a characteristic time of the particular response. E.G. for a particular mode of wing bending the characteristic time is the time which enters into the logarithmic decrement of the oscillation. The problem is furthermore <u>linearized</u>, i.e. the relation between force and response is considered linear. Hence we restrict the input to small fluctuations. This assumption is usually well justified.

We now deal with the problem of finding the response of a linear system with statistically stationary forces. Such a problem can be handled with generalized harmonic analysis. One can introduce power

spectra for the input and output and use the concept of "admittance", "impedance" or "transfer function" to characterize the system. For a given input spectrum and known system, the output spectrum and hence the mean square of the output can be obtained easily.

These concepts were first applied to aerodynamical problems by Clementson (ref. 1) and Liepmann (ref. 2) independently. Since then a large number of papers have dealt with various aspects of the problem (e.g. ref. 3, 4, 5). The first papers considered the problem as a one-dimensional stochastic process (i.e. the angle of attack was considered a random function of time only, spatial variation of α was neglected). The response of the configuration was described by a simple transfer function. Recently the theory has been extended to fluctuations, which like actual turbulence, vary in space and time (i.e. at any given time are not uniform along the span) and account has been taken of the finite span of the wing (ref. 4, 6).

The most interesting part of the "admittance" or "transfer function" of a wing is the "aerodynamic admittance". This aerodynamic admittance relates the angle of attack of a rigid airfoil to the lift. This relation varies with frequency because of the loss of lift due to circulation lag. In ref. 2 Sears' result (ref. 7) for the aerodynamic admittance (i.e. to the lift response for a sinusoidal input) was used to demonstrate the character of the response.

The present experimental investigation was undertaken to study in detail a basic problem in this field, namely the lift of a rigid wing in turbulent air.

Thus the fluctuating lift of a wing in an airstream with known turbulence was measured and analyzed. The results can be compared with the theoretical studies cited above. The experiments are necessary to check on the validity of some of the simplifying assumptions made in the theory. Furthermore the experiments demonstrate the possibility of measuring aerodynamic transfer functions from a study of the response of a configuration in a field of turbulence. There is little doubt that this technique will become very useful in flight testing.

II. Measuring Principles. Definitions.

It has been pointed out that the random nature of the problem allows application of the ideas of stationary stochastic processes. Therefore one would like to measure some of the statistical quantities which define such a process. Specifically the quantities measured are the turbulence spectrum, the airfoil displacement spectrum, the lift curve slope of the airfoil, and the mechanical admittance (frequency response) of the spring system. From these measurements one may find the lift spectrum and the aerodynamic admittance.

Aerodynamic Admittance. For a linear system under stochastic forcing the ratio of the response spectrum to the input spectrum is equal to the absolute square of the admittance.* For the case of an airfoil in a turbulent stream, the lift may be regarded as the response and the fluctuating angle of attack presented by the turbulent stream as the input. The square of the aerodynamic admittance is then equal to the ratio of lift spectrum, $g(\omega)$, to angle of attack spectrum, $f(\omega)$, where $g(\omega)$ and $f(\omega)$ are defined by the following relations:

$$\overline{\alpha^2} = \int_0^\infty f(\omega)\, d\omega \qquad (\overline{\alpha^2} \text{ signifies mean square angle of attack})$$

$$\overline{L^2} = \int_0^\infty g(\omega)\, d\omega$$

If $\phi(\omega)$ denotes the complex aerodynamic admittance then

---

* See reference 2.

$|\phi|^2$ is related to $f(\omega)$ and $g(\omega)$ by:

$$g(\omega) = |\phi|^2 f(\omega) \qquad (1)$$

w Turbulence Spectrum. If w denotes the component of fluctuating turbulent velocity in the direction of the lift vector, then the fluctuating angle of attack is given approximately by $\alpha(t) = \frac{w}{U}$. The w spectrum of turbulence is measured by putting the output from a w-sensitive hot wire anemometer into a wave analyser as explained on page 13.

Lift Spectrum. The lift spectrum must be found indirectly, since in the experiment only the displacement of the airfoil is measured. The lift spectrum $g(\omega)$ and displacement spectrum $h(\omega)$ are again related by the mechanical admittance of the spring system which supports the airfoil. The mean square displacement, $\overline{v^2}$, is given by:

$$\overline{v^2} = \int_0^\infty h(\omega)\, d\omega$$

If the mechanical admittance is denoted by $\psi(\omega)$ we have

$$h(\omega) = |\psi|^2 g(\omega) \qquad (2)$$

The displacement spectrum is measured by putting the voltage output from a displacement pick-up into a wave analyser. The absolute

mechanical admittance is found by measuring the displacements which result when the airfoil is driven sinusoidally by means of a coil and magnet at frequencies selected by an oscillator.

Total Admittance. The measured quantities are the mechanical admittance, ψ , the displacement spectrum, $h(\omega)$, and the angle of attack spectrum, $f(\omega)$. One wants to obtain the aerodynamic admittance from this information. The above spectra are related by some total admittance, χ , such that

$$h(\omega) = |\chi|^2 f(\omega) \tag{3}$$

As seen from equations (1), (2), and (3), the total admittance, χ , is just the product of mechanical admittance and aerodynamic admittance.

$$h(\omega) = |\phi|^2 |\psi|^2 f(\omega) \tag{4}$$
$$|\chi|^2 = |\phi|^2 |\psi|^2$$

Therefore the absolute aerodynamic admittance, $|\phi|$, is found from the measured quantities:

$$|\phi| = \frac{1}{|\psi|} \left[\frac{h(\omega)}{f(\omega)}\right]^{1/2} \tag{5}$$

Finite Span Effect. To determine experimentally the effects of finite span, the span has been made adjustable by means of sliding

end plates. The maximum span is fixed by the spanwise dimension of the wind tunnel jet. The minimum span is limited as a consequence of the fact that, since forces are found from displacements, at least a portion of the airfoil must undergo displacement. If the movable portion is a narrow strip of the span then the strip width is the minimum span that can be obtained. This is because the end plates cannot be brought closer together than the strip width without interfering with the motion of the strip.

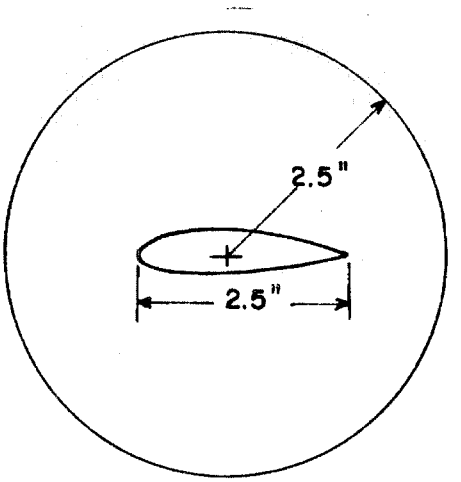

End View

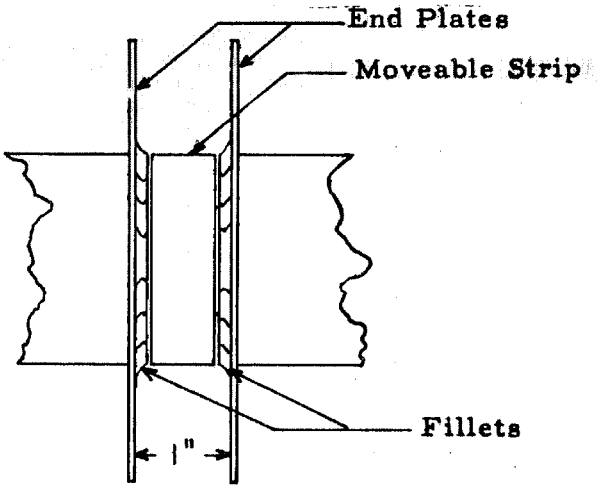

Top View (Minimum Span)

Several considerations limit the strip width. The strip width must be large enough so that (1) the aerodynamic forces are adequate for measurement, (2) gap effects are small. The strip width should be small enough so that the minimum span position approximates the limiting case of two-dimensional turbulence over the strip. If the minimum span is less than the scale of turbulence then three-dimensional effects are sufficiently small so that the two-dimensional case is approximated.

III. Experimental Equipment and Procedures.

Wind Tunnel. The wind tunnel used for the experiments is a low speed tunnel which opens into a free jet at the working section. The original jet size was 7" x 72" but has since been reduced to 7" x 12" in order to increase the maximum velocity. With a turbulence grid in the contraction section the maximum speed is about 65 mph; without the grid the maximum is about 100 mph.

Model Airfoil. The airfoil tested has a 20 per cent thick, symmetrical section and a 2-1/2" chord. Only a narrow strip (0.7" in span) of the airfoil is movable. The floating strip is located at mid-span as shown in fig. 1.

The small size of chord was chosen for several reasons. First, the jet is small and consequently the model must be small if tunnel wall corrections are to be kept small. Second, the theory assumes that the turbulence pattern does not change as the air passes over the chord. This requirement can be approximated only if the chord is small compared to the distance over which significant turbulent decay takes place. Finally, to obtain adequate response the chord should not be large compared to the scale of turbulence, and the scale of turbulence is limited by the jet dimensions and the grid size.

Force Measurements. Due to the small size of the airfoil it did not seem feasible to measure forces by means of pressure

pickups. Therefore it was decided to find forces from displacement measurements. The floating strip, upon which forces are to be found, must be constrained to small displacements if a rigid airfoil is to be simulated. Consequently the floating strip is supported by a relatively stiff spring system. Because of the small size of the airfoil there was not space to mount supporting springs next to the strip, so it was necessary to put the spring system outside the airfoil (figs. 1 and 2). A beam, whose stiffness is much greater than that of the supporting springs, carries the load from the floating element to the springs. The beam lies inside a slot in the fixed dummy airfoil. The spring system consists of parallel flexure links which constrain the motion to simple plunging.

Pickup. The displacement pickup is a small differential transformer (Schaevitz Gage)* One hundred k.c. exciter current, supplied to the transformer coil by a crystal oscillator, is modulated by an iron core which moves with the airfoil (fig. 1). The modulated signal is then demodulated and put into a wave analyser, filter or integrator.

Spectrum Measurements. Three frequency ranges may be distinguished according to the instrument used for the spectrum measurements. Above approximately 70 c.p.s. a Hewlett-Packard wave analyser is used. A Krohn-Hite Low Pass Filter covers the frequency range from 2 - 10 c.p.s. Spectrum points between 10 and 70 c.p.s. may be found by using the mechanical resonance of the

---

* See Schaevitz Engineering (Camden, New Jersey) Catalog.

airfoil spring system as the filter. This latter method is discussed in detail on page 14.

Integrator. The large fluctuations of the response make it necessary to use some kind of integrator in order that some average R.M.S. value can be obtained. For this purpose a resistance-capacitance circuit whose time constant is 17-1/2 minutes is used. Measurements of total response require about a 10 min. averaging time to get less than 5 per cent scatter.

Mechanical Admittance. It was at first believed that the mechanical admittance could be computed by assuming the spring system to be a one degree of freedom damped oscillator. The motion would then be described by the equation:

$$mv + \beta \dot{v} + Gv = F(t)$$

and the absolute admittance given by:

$$|\psi| = \frac{1}{(m^2(\omega^2 - \omega_o^2)^2 + \beta^2\omega^2)^{1/2}}$$

This simplified picture proved to be inadequate because in addition to the natural frequency of the parallel link system, a mode of oscillation involving the beam in bending appeared in the response spectrum. Therefore it seemed necessary to find the mechanical admittance experimentally.

The mechanical admittance is found by measuring the displacement as a function of frequency for a driving force of constant

amplitude. For this purpose a coil, carrying an amplified oscillator signal, is attached rigidly to the end of the beam. The coil lies in the field of a permanent magnet of strength B, so that the force exerted on the coil when it carries current i , is just $\vec{F} = \vec{i} \times \vec{B}$ (if the frequency is not too high).

Details of the arrangement are shown in fig. 2. The coil is aligned in the circular air gap of the magnet by means of a cylindrical spacer which is pulled out of the gap when the cement which bonds the coil to the beam has set.

To find the point at zero frequency, d.c. current is put through the coil. The point at zero frequency is essential because one wants to compare the dynamic response of the airfoil at each frequency to the static lift of the airfoil.

Lift Curve Slope. Since for admittance measurements the dynamic response at each frequency is referred to the static lift of the airfoil, the lift curve slope is measured. This is done by rotating the airfoil in the flow. The force one measures is actually the normal force but this force is very nearly equal to the lift for small angles of attack. The lift curve slope is measured with the grid in the tunnel, since without the grid the slope is about 20 per cent larger and also laminar separation causes the lift curve to bend over at about 6°. The lift curve slope of the airfoil is of slope per radian about 4. No appreciable change with Reynolds Number occurs for the range of Reynolds Number considered (~ 80,000 - 150,000). The lift curve is plotted in figure 3.

Selection of Spring Stiffness. The parallel flexure links, which comprise the spring system, must be stiff enough to restrict the motion to small displacements in order that (1) the airfoil motion shall not modify the flow field (2) aerodynamic damping shall be small. An instrument which is capable of measuring sufficiently small displacements (fluctuating or static) is the differential transformer mentioned on p. 9. The instrumentation is designed to allow a maximum displacement of 0.004" in low sensitivity position and a maximum of 0.001" in high sensitivity position. In selecting the spring stiffness the maximum linear range of the pickup determines the upper limit of deflection, whereas the signal to noise ratio determines the lower limit.

For design purposes it is satisfactory to assume a one degree of freedom system: $mv + \dot{v} + Gv = F(t)$. Now consider how much each parameter can be varied. A minimum mass is fixed by the spring-beam arrangement shown in fig. 1. If no artificial damping is introduced, the structural damping of the flexure links is the definitive damping of the system. An estimate of the forces can be obtained from the theory. From the above information a fair guess can be made of suitable values of spring constant, G. The dimensions of the flexures which will give this spring constant can then be computed.

Turbulence Spectrum. Turbulence is created in the airstream by means of a grid upstream of the airfoil. To find the fluctuating angle of attack which the airfoil experiences due to the turbulent

stream one must find the velocity fluctuations in the direction of the lift vector. Denoting this velocity component of the turbulence by w and the mean speed by U, we have for w small compared to U an angle of attack given by:

$$\alpha(t) = \frac{w}{U}$$

w may be measured by hot wire anemometry. Two hot wires are placed close together in the flow such that both wires lie in planes parallel to the plane of w and U. The resistance of a hot wire and consequently the voltage across it, is a function of wire temperature. The wire temperature depends upon the component of velocity normal to the wire. Hence if one wire is at angle θ ($\theta = 45^{\circ}$ and $\theta = 60^{\circ}$ were both used) and the other at $-\theta$ to the free stream direction, each wire will have the same voltage drop so that the voltage difference between the two wires will be zero. Thus this configuration of hot wires is sensitive only to the w velocity component. The w-meter may be calibrated either by rotation in a uniform stream, recording voltage difference as a function of angle, or by comparison with standard turbulence grids.

The wire sizes used were 1/10 mil platinum-rhodium and 1/20 mil platinum. There are several advantages in using such fine wires. First the time constant is sufficiently short so that no compensation for thermal lag is necessary over the range of frequencies considered. Also the sensitivity of the fine wires is large enough so that the signal can be put directly into a wave

analyser. No pre-amplification is needed so one source of noise is eliminated. A disadvantage of using very fine wires, especially 1/20 mil platinum, is that they are easily broken or bent out of shape by dust particles in the flow. The w-meter is calibrated before and after each run to determine if the wires have been bent during the run.

Two different grids were used in order to vary the scale of turbulence. The small grid is made of 1/4" diameter wooden dowel rod with horizontal rods spaced 1" apart and vertical rods spaced 1" (i.e. mesh size, M, equals 1). The large grid is of 1/2" diameter dowel with horizontal rods spaced 3" apart and vertical rods spaced 2" apart.

The scale of turbulence is found from the intercept of the u-spectrum of turbulence (u being the fluctuating component of velocity in the stream direction) as shown in appendix I. For the small grid the scale is $\lambda_x \approx 1/2"$ and for the large grid $\lambda_x \approx 1"$.

Using Spring System as a Mechanical Filter. The resonance peak of the undamped spring system is so sharp that nearly all of the area under the mechanical admittance curve is contained within a frequency range of a few cycles (fig. 4). This fact suggests the possibility of using the spring system as a mechanical filter. The mean square displacement, $\overline{v^2}$, is given by integration of equation (4) over all frequencies:

$$h(\omega) = |\phi|^2 \, |\psi|^2 \, f(\omega) \qquad (4)$$

$$\overline{v^2} = \int_0^\infty h(\omega) \, d\omega = \int_0^\infty |\phi|^2 \, |\psi|^2 \, f(\omega) \, d\omega \qquad (6)$$

where ψ is the mechanical admittance and ϕ the aerodynamic admittance. Since ψ has a sharp peak at the natural frequency, ω_o, whereas ϕ and $f(\omega)$ are comparatively slowly varying functions, one may write:

$$\overline{v^2} \approx |\phi(\omega_o)|^2 \, f(\omega_o) \int_0^\infty |\psi|^2 \, d\omega$$

Hence to find the absolute aerodynamic admittance, $|\phi(\omega_o)|$, one measures the total response, $\overline{v^2}$, the turbulence spectrum at ω_o, $f(\omega_o)$, and computes the area, A, under the square of the mechanical admittance curve: $\int_0^\infty |\psi|^2 \, d\omega = A$.

Then

$$\sqrt{\overline{v^2}} = |\phi(\omega_o)| \, \sqrt{f(\omega_o) \, A}$$

$$|\phi(\omega_o)| = \sqrt{\frac{\overline{v^2}}{f(\omega_o) \, A}} \quad \text{(See Appendix II)} \qquad (7)$$

Hewlett-Packard Wave Analyser. The turbulence spectrum above 30 c.p.s. and the displacement spectrum above about 70 c.p.s. are measured on a Hewlett-Packard Model 200A harmonic wave analyser. This analyser has an adjustable half band width from 30 to 145 c.p.s. where the half band width is defined as the number of cycles off resonance at which a given signal is attenuated 40 db. Only the 30 c.p.s. half band width is used, since only comparatively low frequencies

are of interest. Measurements of displacement spectrum could not be made to as low a frequency as for the turbulence spectrum because the turbulence spectrum is quite flat at the low frequency part of the spectrum while the displacement spectrum has a sharp peak (at the natural frequency). Since, in measuring a continuous spectrum with the analyser, one assumes the spectrum is flat or at least linear over the pass band of the analyser, points of the displacement spectrum may be obtained only so long as the analyser pass band does not include a portion of the spectrum which has large curvature (such as occurs when the band width overlaps the resonance peak). For example, the displacement spectrum for the spring system whose natural frequency is 34 c.p.s. is sufficiently flat at frequencies above about 70 c.p.s. to allow accurate spectrum measurement with a 30 c.p.s. half band width. Sample calculation is given in Appendix III.

The displacement spectrum is not found for frequencies higher than about 200 c.p.s. because the noise (i.e. extraneous vibrations) to signal ratio is no longer small above 200 c.p.s.

Low Pass Filter. As previously discussed the Hewlett-Packard wave analyser covers the high frequency end of the spectrum and the spring system used as a mechanical filter measures spectral points in the range 10 - 70 c.p.s. To obtain low frequency points (2-10 c.p.s.) a Krohn-Hite Low Pass Filter is used. The filter pass band can be adjusted to any width by means of independently controlled high and low frequency cut-offs. Once a particular band width has been selected, the shape of the pass band may be found by putting an oscillator signal into the filter and varying the frequency while holding

the amplitude constant. However to find the admittance, only the ratio of input to response is needed, so that by using the same pass band for input and response the area under the pass band is divided out and hence does not enter in the admittance computation.

Second Spring System. For a number of reasons it was decided that a new spring system could be designed which would have many advantages over the old system (of fig. 1). The main difficulty encountered with the original system is the instability of the mechanical admittance. The cause of the instability is presumably due to the fact that the flexure links are built up from pieces and occasionally some slippage occurs during vibration at the interfaces of the metal pieces. As a result boundary conditions are changed and a shift occurs in the natural frequencies of the system. The sketch below illustrates the effect of the frequency shift on the admittance curve.

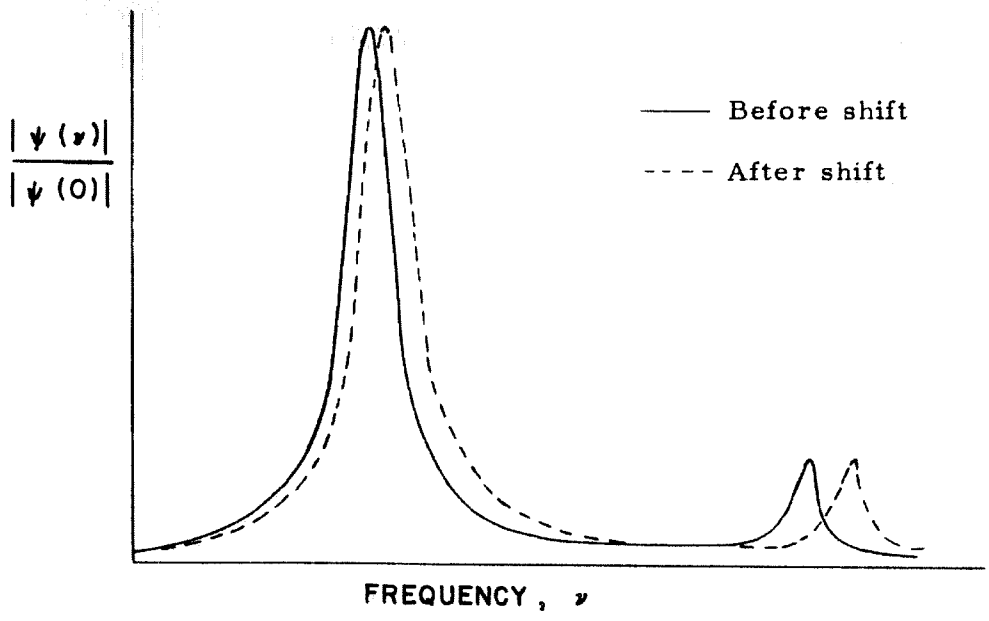

It is noted that a small shift can introduce a large change in the amplitude at any particular frequency. Also a change in the area under the curve usually accompanies the frequency shift. As discussed on page 14 the use of the mechanical system as a filter involves the area under the admittance curve so this area should remain constant. In the new system (fig. 2) frequency instabilities are overcome by machining each flexure link from a single piece of metal. In using the spring system as a filter the natural frequency picks out a single spectral component. Hence one would like to vary the natural frequency in order to get other spectral points. Therefore three sets of flexures were made giving natural frequencies of 17, 34, 68 c.p.s. Intermediate frequencies can be found by screwing threaded brass weights into the hole at the beam c.g. as shown in fig. 2. Also the different maximum amplitudes of deflection which result from the different spring stiffnesses allows the study of aerodynamic damping as a function of airfoil motion.

The symmetry of the new system serves several purposes. First the amplitude of the mode of oscillation involving the beam in bending is less for a symmetrical system. Second, the mechanical admittance obtained by an input at one end of the beam is approximately the same as if the input were applied at the other end of the beam. Therefore one can mount the driving coil at one end of the beam and the strip of airfoil at the other end. This arrangement is a great convenience since the driving unit does not have to be disassembled and reassembled each time one wants to calibrate (i.e. find mechanical

admittance). A disadvantage lies in the fact that sometimes a small metal chip gets lodged between magnet and coil during a run, but this can be discovered by calibrating before and after each run.

Vortex Street Input. As a first step toward a study of the response of an airfoil to a turbulent airstream, it seemed instructive to find the response to a sinusoidal input, since the results could then be compared with the Sears' theory for a rigid airfoil in a sinusoidal gust. To simulate a sinusoidal gust a vortex street was formed by means of a large cylinder upstream of the airfoil. Unfortunately, no wake position could be found for which there was not considerable background turbulence, and consequently a whole spectrum of frequencies was excited. If the street is made small enough so that no background turbulence appears then it is of insufficient strength to excite the airfoil. One might also ask if the shedding frequency could be brought into coincidence with the natural frequency of the spring system, thereby making the response to the vortex street essentially the entire response. Due to the sharpness of the peaks this condition of coincidence is too critical to allow accurate measurement. An example of the displacement spectrum one obtains for the airfoil in the wake of a cylinder is shown in the sketch.

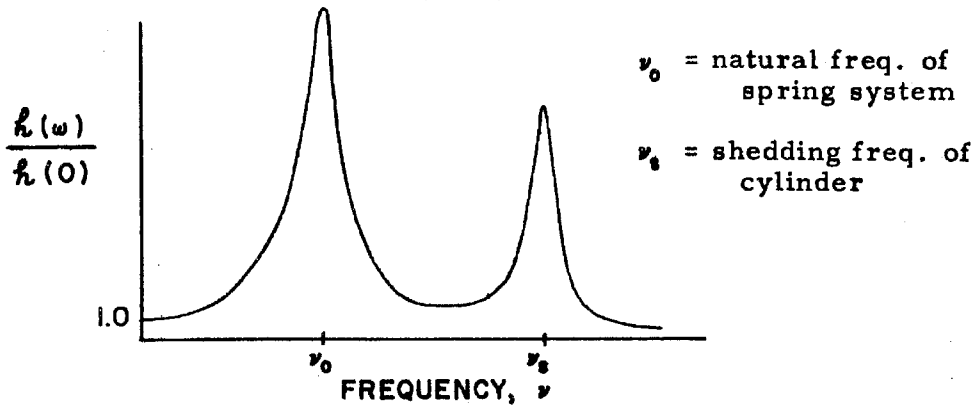

Secondary Flow. When the end plates (page 7) were initially placed one on either side of the movable strip of airfoil, the aerodynamic admittance was found to be larger than $|\phi(0)|$ as the frequency approached zero. The lift as the frequency tends to zero may be less than the static lift (because the angle of attack correlation along the span may be less than 1) but it cannot exceed the static lift. To explain this difficulty it was assumed that some kind of secondary flow occurred between the plates which caused the dynamic response of the airfoil to be too high. A tuft placed in the flow between the plates illustrated that the flow was at least separating rather badly. Fillets were then added at the intersection of plate and airfoil as shown by the sketch on page 7. Again the tuft was placed in the flow; this time no evidence of separation could be found and the aerodynamic admittance was well behaved (i.e. $|\phi(\omega)| \leq |\phi(0)|$, see figs. 5 and 6).

Gap Effect. To determine the effect of the gaps on either side of the movable strip of airfoil, measurements of the response were made with the gaps covered by micro-film.* The film was found to restrain the motion of the strip and so it was necessary to apply the film with the gaps enlarged to about 1/4" and then buckle the film by restoring the gaps to their original width of a few hundreths of an inch. This meant that some end effects would still be present because of the grooves formed by the buckled film, but at least air could not pass through the gaps. The static lift curve slope and the dynamic response of the airfoil were found to be (within the error of measurement) the same as without the film.

---

* As supplied by model airplane shops.

Noise Level. To find how much of a given response measurement is due to extraneous vibrations from the test stand and electrical noise in the instrumentation, the movable strip of airfoil is shielded from the flow. The overall noise level is then simply the shielded reading. The shield is a hollow airfoil section which is large enough to clear the strip airfoil as shown in the sketch below. The noise level was negligible for the measurements reported here.

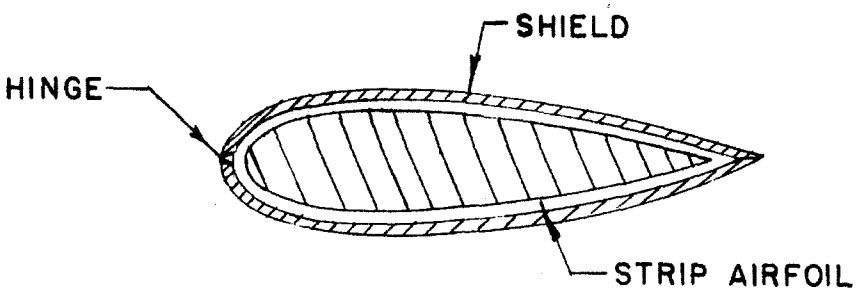

END VIEW

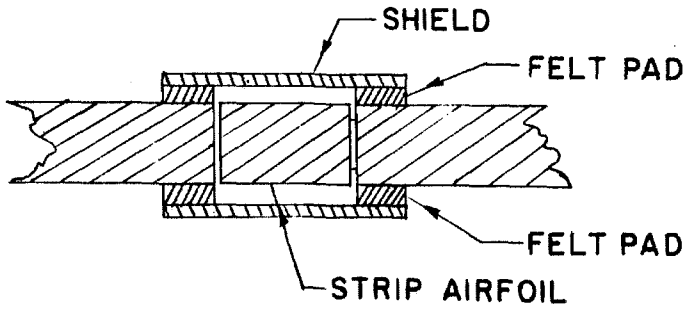

LEADING EDGE VIEW

Damping. One would like to vary the damping of the spring system for several reasons. First, in actual flight conditions the vibrating structure might be predominately damped by either structural damping of aerodynamic damping so that both cases deserve investigation. Second, since the linear range of the Schaevitz gage must simultaneously accommodate amplitudes corresponding to a whole spectrum of displacements, the largest amplitude (i.e. resonance peak) should not be too large compared to the smallest amplitude considered (corresponding to some arbitrary frequency ν_{max}). This is illustrated below.

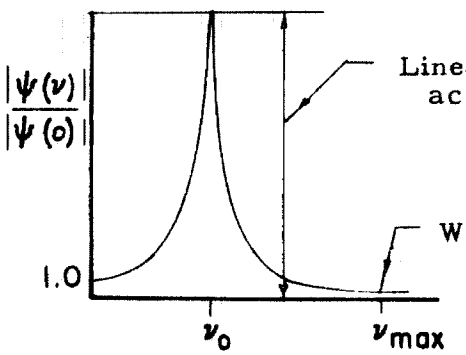

Linear range of Schaevitz - adjusted to accommodate resonance peak

Wave Analyser must measure frequency components of this order. Cannot amplify further or resonance peak exceeds linear range of Schaevitz gage.

β small

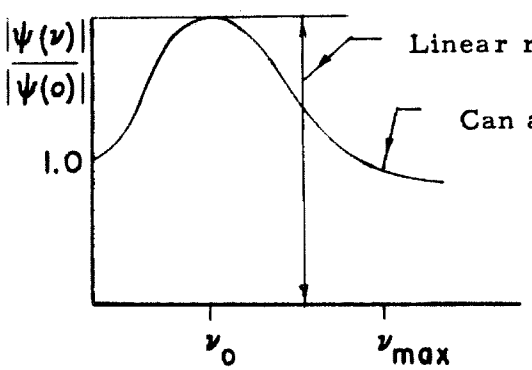

Linear range of Schaevitz

Can amplify the ν_{max} component this much without resonance peak exceeding linear range of Schaevitz gage.

β large

Damping by means of an oil-filled dash pot was attempted but was unsuccessful, as the velocities are too small to be appreciably influenced by this kind of damping. Then an attempt was made to increase the structural damping by painting a rubber compound on the flexure links at the grooves where the bending takes place. The system could be almost critically damped in this way but the deflection was no longer linearly related to the force (at a given frequency).

Finally damping by means of a rubber strip in tension was tried. The force-deflection linearity was restored but some additional modes of vibration appeared which were not very reproducible. Consequently all the data presented are for the undamped system. It is felt, however, that a damped system could be made to work if more time were spent on the problem.

Aerodynamic damping of the airfoil motion was too small to show up in the admittance in all measurements except those involving the largest amplitude of motion (i.e. for the case of the mechanical filter using the weakest springs). For this case the admittance (figs. 5 and 6, $k \approx 0.1 - 0.3$) in general drops somewhat below the curve drawn through the other points. That the effect is more pronounced with increasing mean speed (and hence with increasing displacement amplitude) suggests that aerodynamic damping is the cause.

To check this supposition the mechanical admittance was measured (using set-up shown in fig. 2) with and without a free stream. The mechanical admittance when measured in the free stream was not diminished enough to account for the effect mentioned above; but then

the method of accounting for the aerodynamic damping by calibration is not quite comparable to the actual situation existing in the response to a turbulent flow, since in the former case the driving force is applied at one end of the beam and the damping force at the other, whereas in the latter case all forces are applied at one end of the beam.

IV. Results

Infinite Wing. The essential results of the measurements are plotted in figs. 5 and 6. Two sets of data are given in each figure, one for the wing with end plates, the other for the wing spanning the jet. The distance between the end plates is small enough so that the turbulent fluctuations are nearly correlated across the effective span and hence these sets of data should agree with the admittance function from Sears' theory. This is seen to be true for reduced frequencies larger than about 0.8. For smaller reduced frequencies the measured admittance is well below Sears' curve. This effect is more pronounced for the large grid (fig. 6).

Two reasons are suggested to explain this effect. One is the inhomogeniety of the turbulence at low frequencies. The effect is more pronounced for the large grid because the airfoil is effectively closer to it ($\frac{x}{M} = 8$, for the large grid, whereas $\frac{x}{M} = 20$ for the small grid). A few tentative measurements using the small grid at $\frac{x}{M} = 8$ support this conjecture.

The other reason is that the end plates may not have been large enough (compared to the large eddies that correspond to low frequencies) to completely isolate the portion of the span between the end plates from downwash effects due to the wake arising from the rest of the wing. The data of Hakkinen and Richardson at M.I.T. (ref. 8) are for an essentially infinite end plate size (wing spanning a closed tunnel), and drop off of the admittance curve at low frequencies does not appear.

For the case of the wing spanning the jet it is seen that the entire admittance curve falls far below the Sears values, indicating that three-dimensional effects are very important and that the two-dimensional admittance function is no longer even approximately valid. The admittance for this case (span large compared to scale of turbulence) is nearly frequency independent within at least a range of reduced frequencies from 0.2 to 2.0, the highest value for which data were taken. It is to be emphasized that simply having the span of the movable strip, t_s, less than the scale of turbulence, λ_x, is not sufficient if one is to measure a two-dimensional aerodynamic admittance. The ratio of total span s, to scale λ_x will always enter.

To clarify the nature of the three-dimensional effects, assume the general problem (in which the turbulence presents an angle of attack $\alpha = \alpha(y,t)$ to the wing) to be composed of two simpler problems, (1) $\alpha = \alpha(t)$ only and (2) $\alpha = \alpha(y)$ only. The first case is treated in two-dimensional non-stationary theory (e.g. ref. 2, 7). The second case may be represented by Prandtl's horseshoe vortex concept, in which downwash due to the wake is calculated from the Biot Savart Law. From this consideration of the wake effect it is apparent that even if the span of the movable strip, t_s, is small compared to the scale λ_x, wake effects from the entire span s will contribute to the response of the strip. This is seen in the experimental data (fig. 5 and 6)--a large difference in the aerodynamic admittance results from using two different values of span s (i.e. with and without end plates) while keeping scale λ_x and strip span t_s fixed.

Aspect Ratio Effect. Due to instrumentation difficulties and other unexpected problems arising in the experimental determination of the aerodynamic admittance for a two-dimensional wing, there has been little time remaining for investigating the case of a finite aspect ratio wing in turbulent flow. However the few measurements which are discussed below give some indication of the qualitative behavior of the response with changing aspect ratio.

For a constant turbulence level and mean speed, the response of the movable strip for several aspect ratios is given, first for the strip located near the wing root and second, for the strip near the wing tip. The relative position of the movable strip and the aspect ratio of the wing may be adjusted by means of a sliding end plate on the inboard side of the strip and by changing the span of the outboard portion of wing. The portion of wing outboard of the movable strip is supported by two rods which extend from the inboard dummy airfoil through clearance holes in the movable strip to the outboard section.

The static and dynamic response of the strip near the wing root for the following configurations is summarized in the chart below.

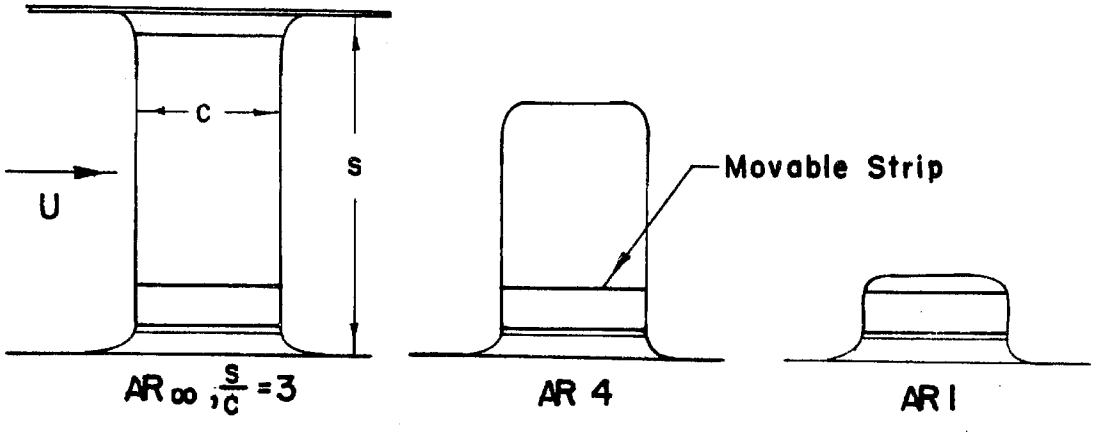

Aspect Ratio	Values of $\sqrt{L^2}/\sqrt{L_\infty^2}$		
	Static	3 cps	17 cps
∞	1	1	1
4	0.89	1.25	1.48
1	0.5	1.04	1.23

$\sqrt{L_\infty^2}$ = R.M.S. lift for the infinite aspect ratio wing

It should be noted that the configuration denoted by AR_∞ is of infinite aspect ratio only with regard to tip effects—it is of span s with regard to the response to turbulence.

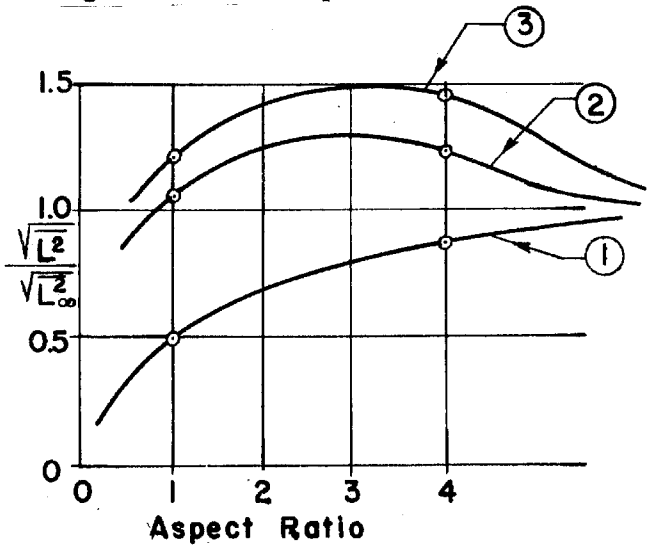

1. Static Response of Root Element
2. 3 cps Response of Root Element
3. 17 cps Response of Root Element

The curves approach 1.0 as $AR \to \infty$

Curve (1) shows that the static response is monotonically diminished due to tip effects as the aspect ratio is decreased. Curves (2) and (3) show that the dynamic response of the root element at first increases as the span is reduced, then decreases. This is because as the span (and hence the wake) is shortened the cancelling effect due to the wake is reduced (see page 26). As the aspect ratio is further reduced the tip effect becomes predominant causing the response to diminish.

Response of the strip near the wing tip is given below:

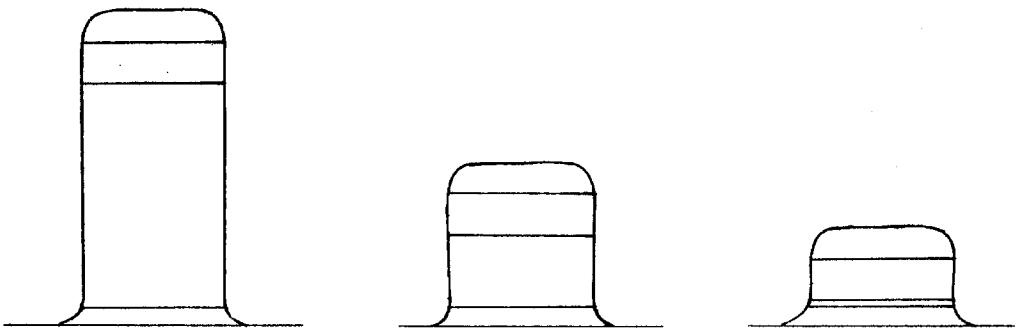

Aspect Ratio	Values of $\sqrt{L^2}/\sqrt{L_4^2}$		
	Static	3 cps	17 cps
4	1	1	1
2	0.95	1.04	1.03
1	0.75	1.12	1.10

$\sqrt{L_4^2}$ = R.M.S. lift for the wing of aspect ratio 4.

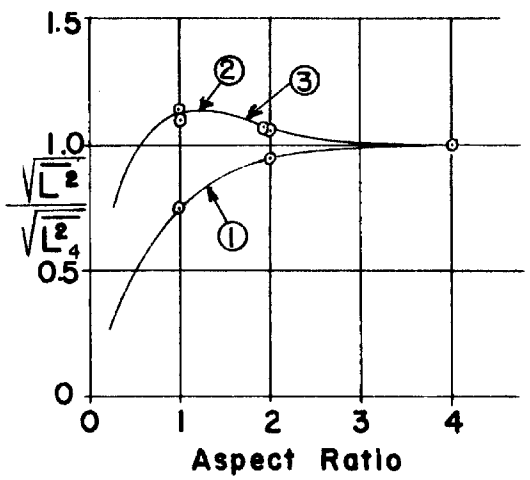

1. Static Response of Tip Element
2. 3 cps. Response of Tip Element
3. 17 cps Response of Tip Element

The curves for the tip element show the same trends as discussed for the root element.

V. Concluding Remarks

a). The aerodynamic admittance of a wing has been obtained from measurements of the lift power spectrum and turbulence spectrum.

b). If end plates are used such that the fluctuations are correlated across the effective span of the wing, the physical situation can be made to approximate the one-dimensional study of Ref. 2. It is then found that the aerodynamic admittance approaches Sears' theoretical curve for reduced frequencies higher than about 0.8. Hence the assumption made in the theory that the influence of the wing on the turbulence can be neglected is borne out by the measurements.

c). The smoothing effect of a wing span large compared to the scale of turbulence is demonstrated. The aerodynamic admittance for the airfoil measured is reduced by a large factor from the case with end plates.

Appendix I.

(a) Scale of Turbulence.

The scale of turbulence is in a sense an average eddy size as may be seen from the way in which it is defined. One may define a time scale, T, of the motion by the area under the autocorrelation curve, where the autocorrelation $f(\tau)$ is defined by $f(\tau)=\overline{u(t)\ u(t+\tau)}$

$$f(0)\ T = \int_0^\infty f(\tau)\ d\tau$$

The length scale, λ_x, is related to T by,

$$\lambda_x = UT$$

So that,

$$\lambda_x = U\ \frac{\int_0^\infty f(\tau)\ d\tau}{f(0)}$$

To writethis expression in terms of the power spectrum, one may use the well known relation:

$$f(\omega) = \frac{2}{\pi} \int_0^\infty f(\tau) \cos \omega\tau\ d\omega$$

$$\therefore\quad f(0) = \frac{2}{\pi} \int_0^\infty f(\tau)\ d\tau$$

Similarly from the equation

$$f(\tau) = \int_0^\infty f(\omega) \cos \omega\tau\ d\omega$$

one obtains

$$\mathcal{f}(0) = \int_0^\infty f(\omega)\, d\omega$$

Hence

$$\lambda_x = U \frac{\pi}{2} \frac{f(0)}{\int_0^\infty f(\omega)\, d\omega}$$

For example, for U = 92 ft/sec, the u-spectrum of turbulence for the large grid gives:

$$\frac{f(0)}{\int_0^\infty f(\omega)\, d\omega} = 5.8 \times 10^{-4} \text{ seconds}$$

$$\therefore \quad \lambda_x = 92 \text{ ft/sec} \times \frac{\pi}{2} \times 5.8 \times 10^{-4} \text{ sec} = 0.084 \text{ ft}$$

$$\lambda_x \approx 1"$$

Appendix II

Sample Calculation.

Using the mechanical system as a filter to find the response at a frequency, ω_o, and the wave analyser to find the input at this frequency, one may compute the absolute aerodynamic admittance $|\phi|$.

From equation (7) page 16, $|\phi(\omega_o)|$ is given by

$$|\phi(\omega_o)| = \frac{[\overline{v^2}]^{1/2}}{[A]^{1/2}} \quad \frac{1}{[f(\omega_o)]^{1/2}} \qquad (7)$$

At a natural frequency corresponding to $k = 0.21$, the R.M.S. response of the airfoil (no end plates) to turbulence created by the large grid is

$$[\overline{v^2}]^{1/2} = 0.18 \text{ volts}$$

At $k = 0.21$ the input (obtained by putting the w-meter signal into the wave analyser) is

$$[f(\omega_o)]^{1/2} = 0.33 \text{ degrees}$$

(The actual analyser reading is in volts, but the w-meter is calibrated in volts/degree, hence the input spectrum defined by $\overline{a^2} = \int_o^\infty f(\omega)\, d\omega$ is expressed in degrees.)

Since the input and response are not measured by the same pass band, the pass band areas must be taken into account. The area, A, under the square of the mechanical admittance curve is (fig. 4)

$$A = 4850 \rho$$

The area, A, under the square of the Hewlett-Packard pass band (assumed equal to unity in the derivation of eq. (7)) is

$$A_1 = 11\,\nu$$

Hence the area ratio is: $\frac{4850\,\nu}{11\,\nu} = 440$

So that eq. (7) gives

$$|\phi(\omega_o)| = \frac{0.18 \text{ volts}}{[440]^{1/2} \times 0.33 \text{ degrees}} = .026 \text{ volts/degree}$$

$|\phi(\omega_o)|$ may be put into non-dimensional form, $|\phi_1(\omega_o)|$. At a given airspeed U, rotation of the airfoil in the flow gives the static calibration:

$$|\phi(0)| = \frac{dv}{d\alpha} = 0.10 \text{ volts/degree}$$

$$|\phi_1(\omega_o)| = \frac{|\phi(\omega_o)|}{|\phi(0)|} = \frac{.026 \text{ volts/degree}}{0.10 \text{ volts/degree}}$$

$$|\phi_1(\omega_o)| = .26 \qquad k = 0.21$$

Appendix III

Sample calculations.

Using the Hewlett-Packard Wave Analyzer to find input and response spectra, one may compute the absolute aerodynamic admittance as shown below. At a reduced frequency $k = 1.95$ the R.M.S. response of the airfoil (no end plates) to turbulence created by the large grid is,

$$[h(\omega)]^{1/2} = 0.10 \text{ volts}$$

The input spectrum at $k = 1.95$ is

$$[f(\omega)]^{1/2} = .29 \text{ degrees}$$

The mechanical admittance is,

$$\left|\frac{\psi(\omega)}{\psi(0)}\right| = .33$$

Hence from eq. (5) page 6

$$|\phi(\omega)| = \frac{1}{\left|\frac{\psi(\omega)}{\psi(0)}\right|} \quad \left[\frac{h(\omega)}{f(\omega)}\right]^{1/2} = \frac{1}{.33} \ \frac{.010 \text{ volts}}{.29 \text{ degrees}} = .105 \text{ volts/degree}$$

As in Appendix II, $|\phi(\omega)|$ may be put into non-dimensional form by using the static calibration:

$$|\phi(0)| = \frac{dv}{d\alpha} = .50 \text{ volts/degree}$$

$$|\phi_1(\omega)| = \frac{|\phi(\omega)|}{|\phi(0)|} = .21 \quad \text{at} \quad k = 1.95$$

References.

1. Clementson, G.C.: An Investigation of the Power Spectral Density of Atmospheric Turbulence. MIT, Ph.D. Thesis, 1950.

2. Liepmann, H.W.: On the Application of Statistical Concepts to the Buffeting Problem. JAS, v. 19, December, 1952.

3. Fung, Y.C.: Statistical Aspects of Dynamic Loads. JAS, v. 20, May, 1953.

4. Diederich, F.W.: The Response of an Airplane to Random Atmospheric Disturbances. CIT, Ph.D. Thesis, 1954.

5. Press, H. and Mazelsky, B.: A Study of the Application of Power-Spectral Methods of *General Harmonic Analysis* to *Gust Loads* on Airplanes. NACA TN 2853, January, 1953.

6. Liepmann, H.W.: Extension of the Statistical Approach to Buffeting and Gust Response of Wings of Finite Span. JAS, v. 22, March 1955.

7. Sears, W.R.: Some Aspects of Non-Stationary Airfoil Theory and its Practical Application. JAS, v. 8, January, 1941.

8. Hakkinen, R.J. and Richardson, A.S., Jr., A Theoretical and Experimental Investigation of Random Gust Loads. Part I. Theoretical Analysis and Experimental Results of Aerodynamic Transfer Function of a Simple Wing Configuration in Incompressible Flow. Part II. Theoretical Analysis of Atmospheric Gust Response; Formulation of the Problem and Some Results for Simplified Cases. MIT.

9. Lawson and Uhlenbeck, Threshold Signals, M.I.T. Radiation Laboratory Series, vol. 24 (1947).

10. James, Nichols, and Phillips, Theory of Servomechanisms, M.I.T. Radiation Laboratory Series, vol. 25 (1947).

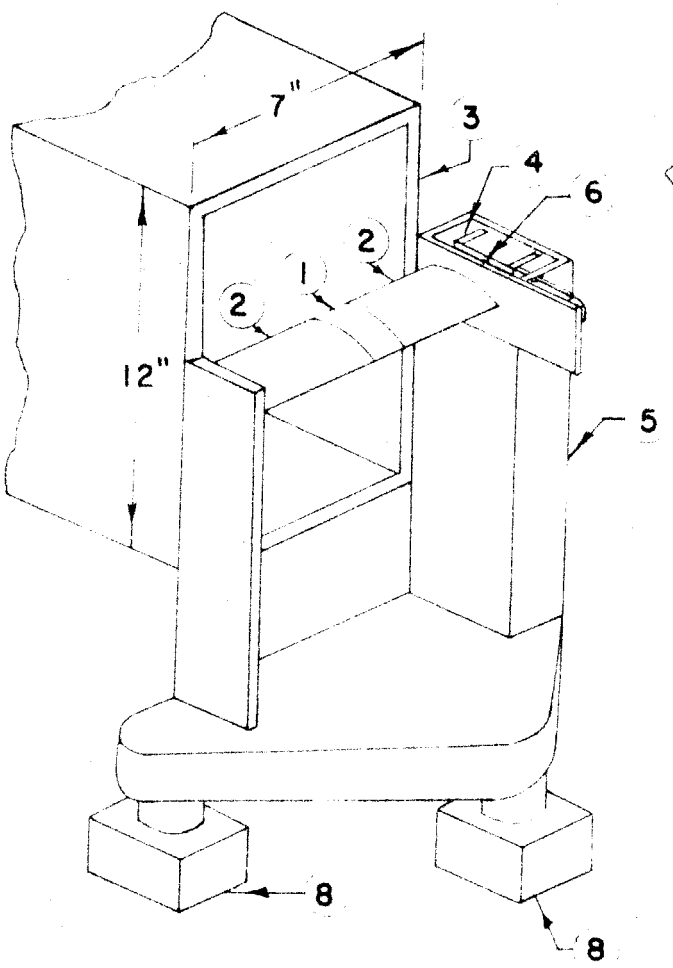

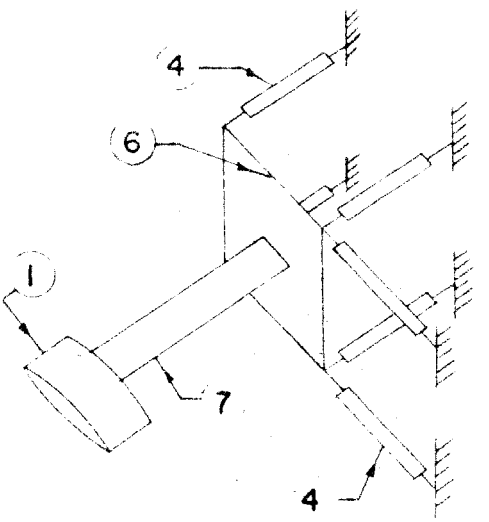

Schematic Drawing of Spring System

1	Moveable Strip
2	Dummy Airfoils
3	Wall of Wind Tunnel Jet
4	Flexure Links
5	Steel Support Structure
6	Location of Displacement Pickup
7	Beam
8	Vibration Absorbers (Foam Rubber and Paper Towels)

Fig. 1. Sketch of Test Setup No. 1.

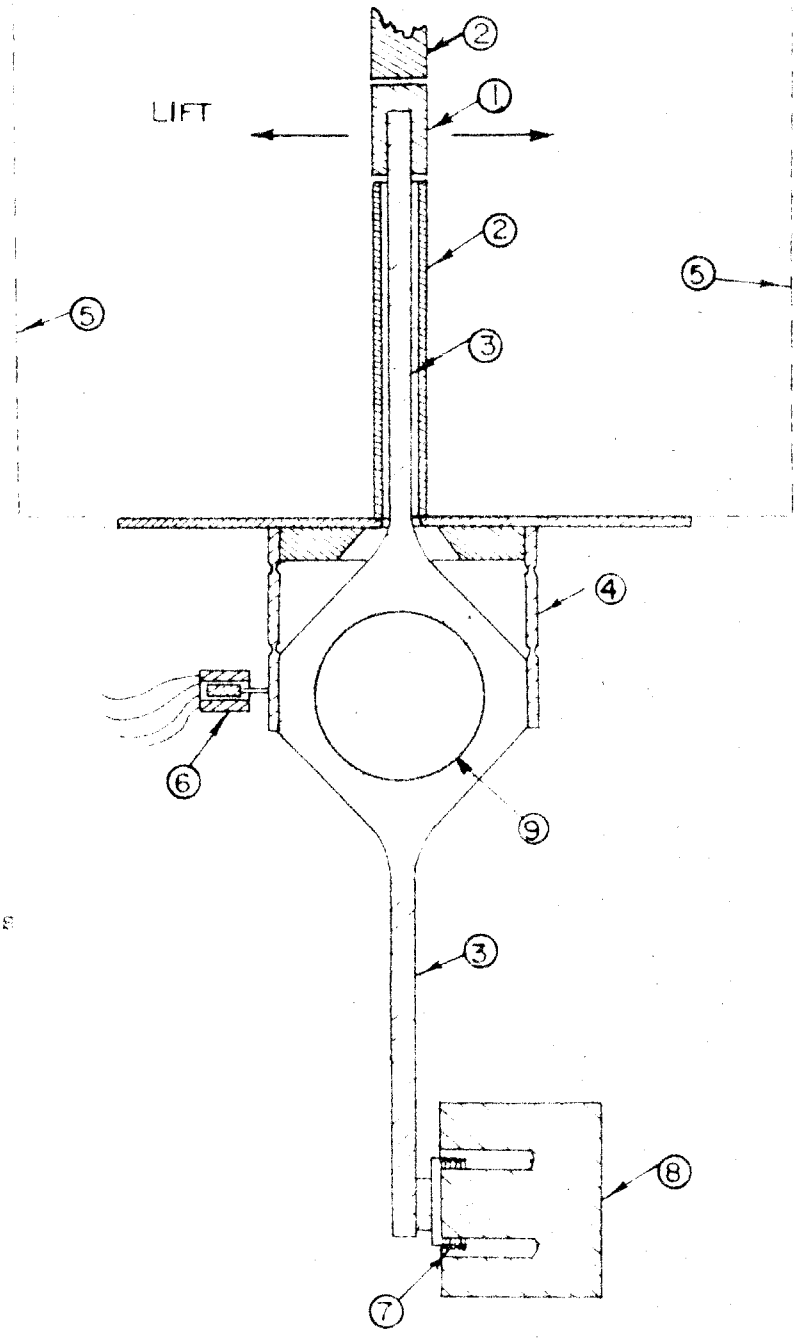

1 Moveable Strip
2 Dummy Airfoils
3 Beam
4 Flexure Links
5 Jet Boundary
6 Schaevitz Gage
7 Coil
8 Magnet
9 Threaded hole for weights

View Looking Upstream

Fig. 3. Section View of Test Setup No. 2

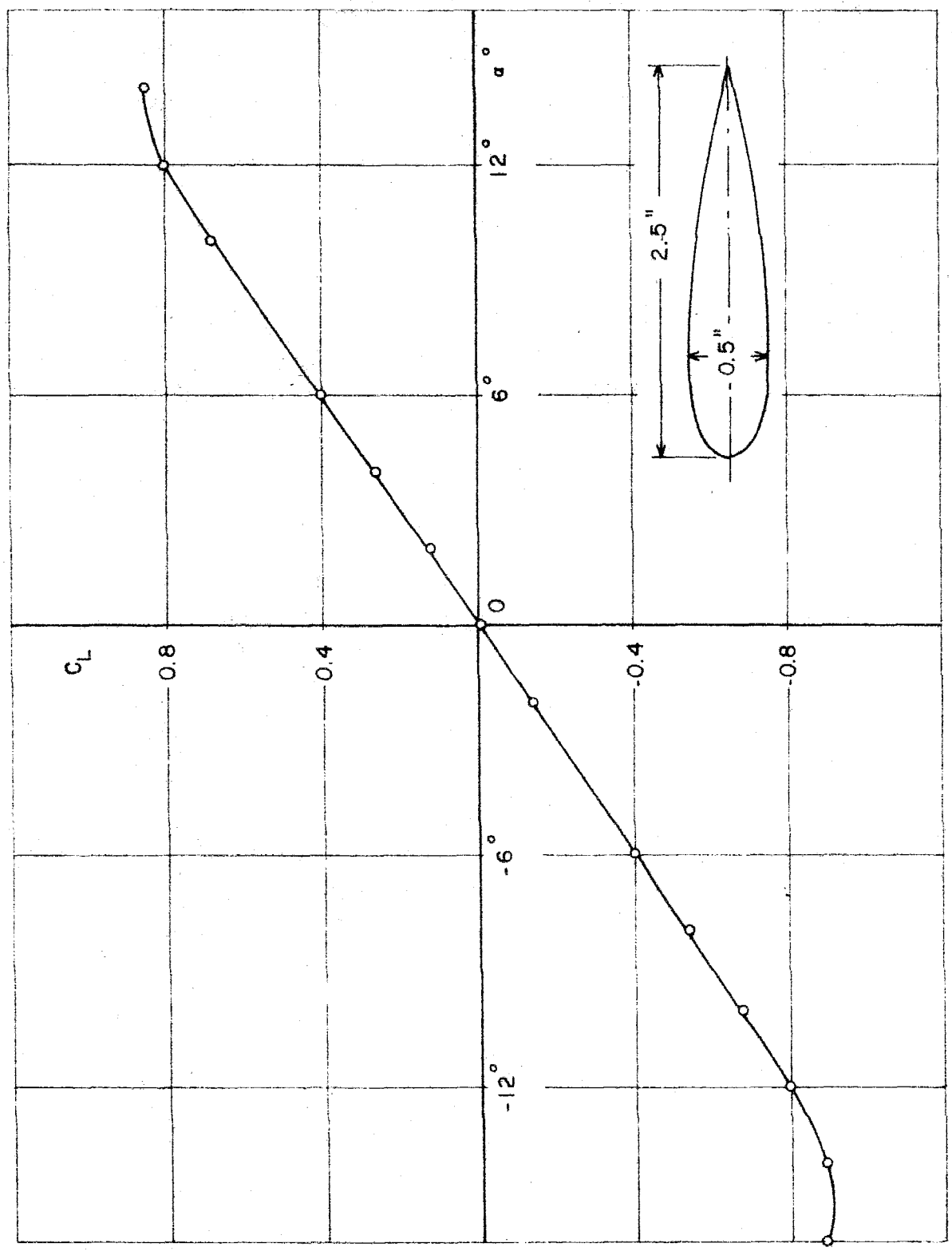

Figure 3. Aircraft Lift Coefficient. Re = 80,000, $C_{L_\alpha} = 0.07 \frac{1}{\text{deg}}$

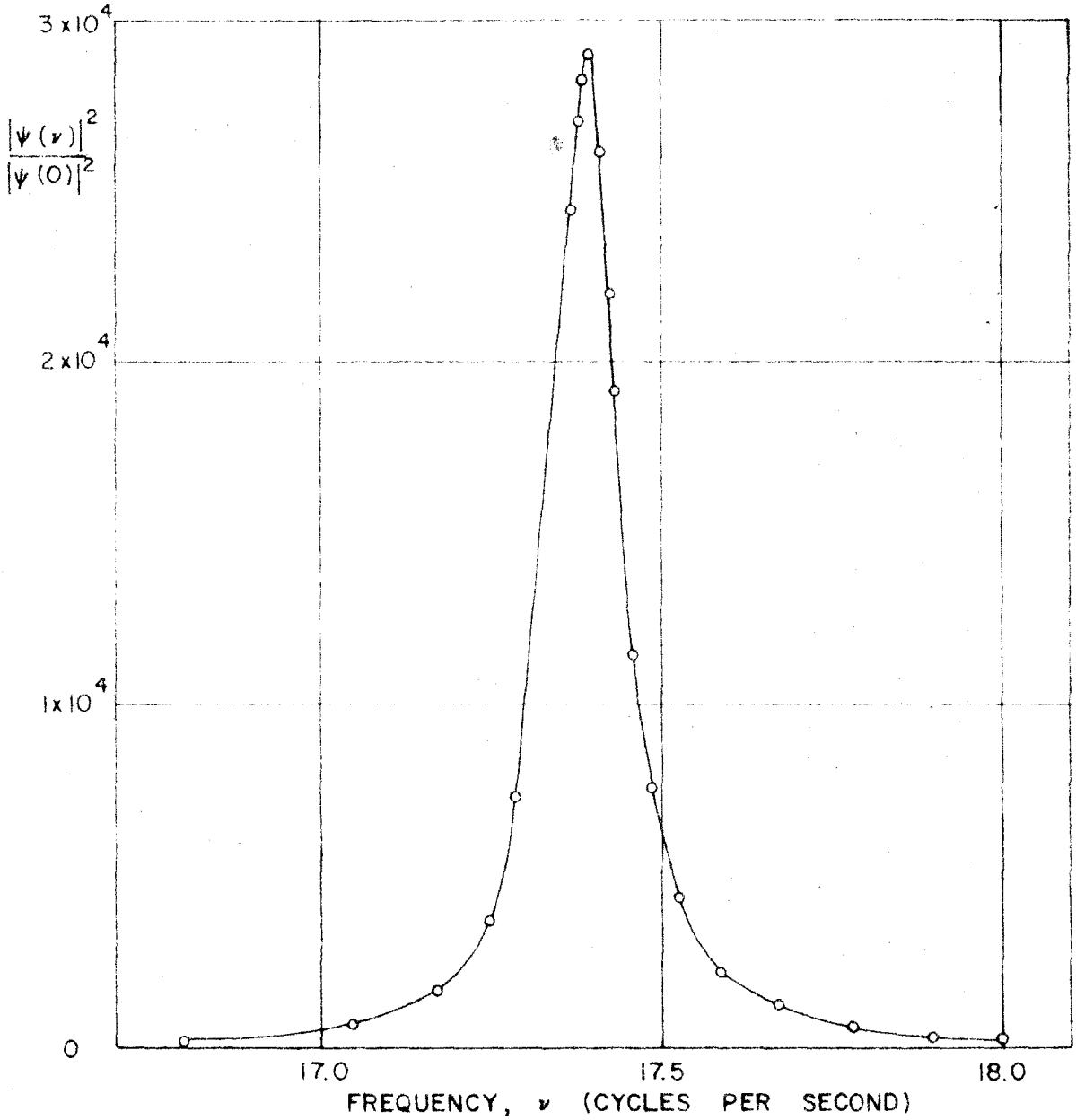

Figure 4. Square of Mechanical Admittance

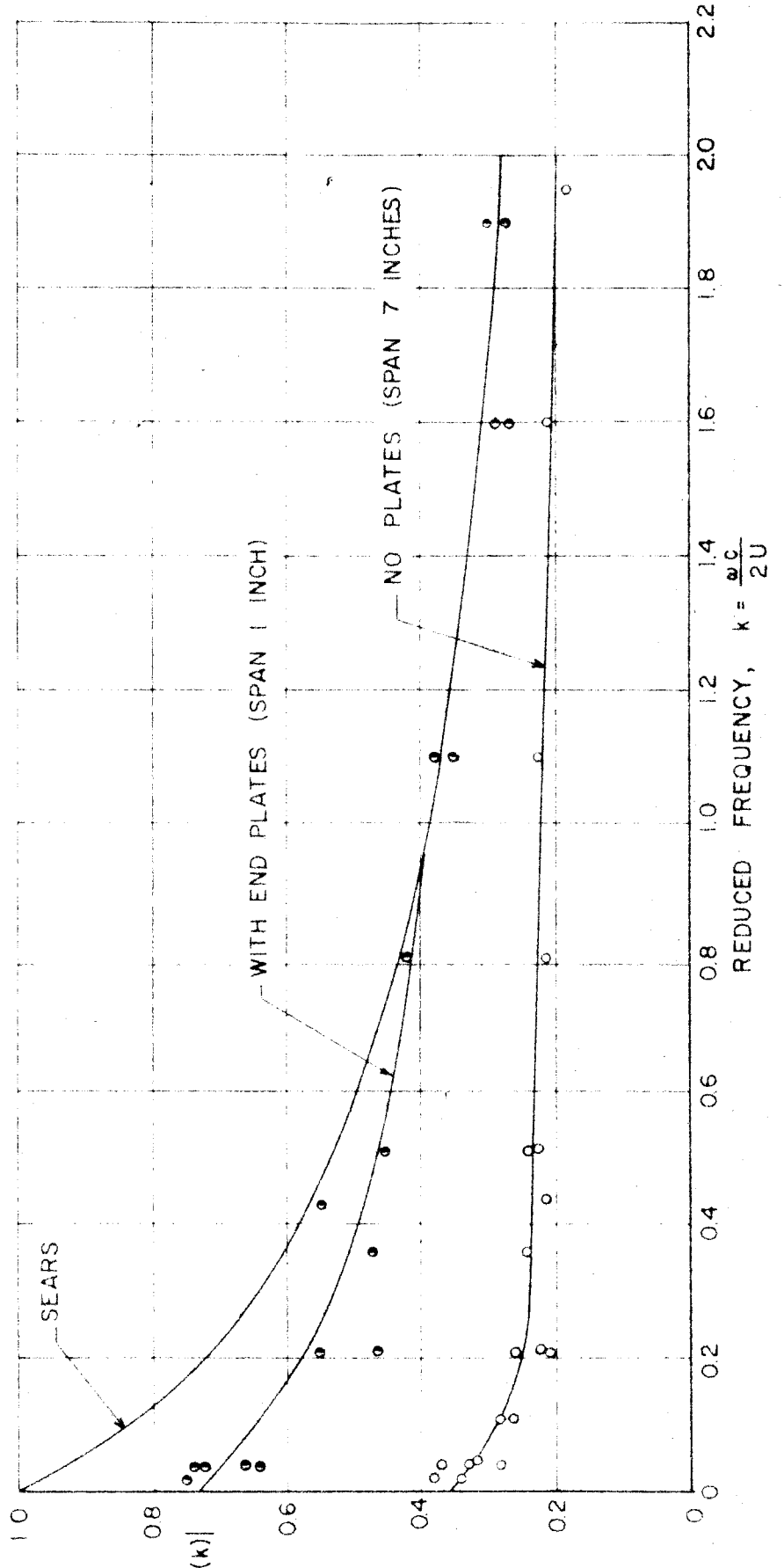

Figure 5. Absolute Aerodynamic Admittance, $|\phi_1(k)|$ Small grid ($M \approx 1$, $\frac{x}{M} \approx 20$, $\lambda_x \approx 1/2''$)

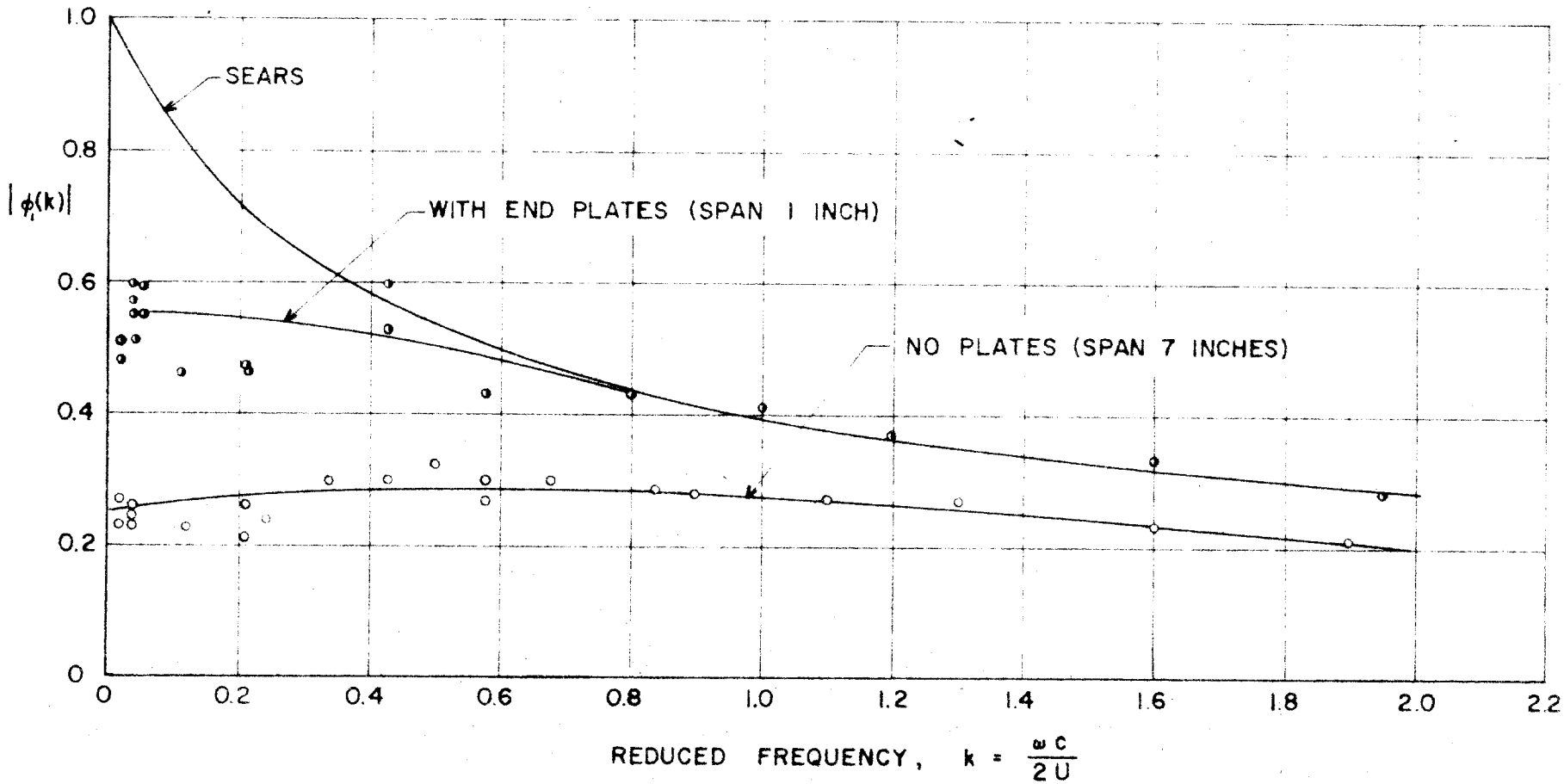

Figure 6 Absolute Aerodynamic Admittance $|\phi_i(k)|$ Large grid ($M \approx 2.5$, $\frac{x}{M} \approx 8$, $\lambda_x \approx 1''$)